Achieving the Optimal Diversity-vs-Multiplexing Tradeoff for MIMO Flat Channels with QAM Space-Time Spreading and DFE Equalization

Abdelkader Medles

Bell Labs, Wireless Research
Lucent Technologies
The Quadrant, Stonehill Green
Swindon, SN5 7DJ, UK

Email: medles@lucent.com
Tel: +44 1793 776783
Fax: +44 1793 776725

Dirk T.M. Slock

Eurecom Institute
2229 route des Crêtes, B.P. 193
06904 Sophia Antipolis Cedex, FRANCE

Email: slock@eurecom.fr
Tel: +33 4 9300 2606
Fax: +33 4 9300 2627

Abstract

The use of multiple transmit (Tx) and receive (Rx) antennas allows to transmit multiple signal streams in parallel and hence to increase communication capacity. We have previously introduced simple convolutive linear precoding schemes that spread transmitted symbols in time and space, involving spatial spreading, delay diversity and possibly temporal spreading. In this paper we show that the use of the classical MIMO Decision Feedback Equalizer (DFE) (but with joint detection) for this system allows to achieve the optimal diversity versus multiplexing tradeoff introduced in [1], when a Minimum Mean Squared Error (MMSE) design is used. One of the major contributions of this work is the diversity analysis of a MMSE equalizer without the Gaussian approximation. Furthermore, the tradeoff is discussed for an arbitrary number of transmit and receive antennas. We also show the tradeoff obtained for a MMSE Zero Forcing (ZF) design. So, another originality of this paper is to show that the MIMO optimal tradeoff can be attained with a suboptimal receiver, in this case a DFE, as opposed to optimal Maximum Likelihood Sequence Estimation (MLSE).

Index Terms:. MIMO transmission, diversity-vs-multiplexing tradeoff, linear precoding, QAM constellations, decision-feedback equalization.

Abdelkader Medles was with the Eurecom Institute, he is now with Lucent Technologies.

The Eurecom Institute's research is partially supported by its industrial members: Bouygues Télécom, Fondation d'Entreprise Groupe Cegetel, Fondation Hasler, France Télécom , Hitachi, Sharp, ST Microelectronics, Swisscom, Texas Instruments, Thales.

I. Introduction

The diversity degree is (currently) defined as the asymptotic slope of the error probability curve at high Signal-to-Noise Ratio (SNR). So it can be enjoyed with a fixed symbol constellation at high SNR. On the other hand, if the SNR is increasing, the channel capacity increases and can be taken advantage off by increasing the rate via an adaptive modulation. However, the work by Zheng and Tse [1] showed that both high SNR benefits cannot be enjoyed simultaneously and a compromise must be accepted. An optimal diversity-vs-rate tradeoff exists. In the context of Multi-Input Multi-Output (MIMO) transmission, this is also called the diversity-vs-multiplexing tradeoff since MIMO systems allow to increase the rate through spatial multiplexing. The optimal tradeoff for frequency flat MIMO channels has been derived in [1], together with a proper positioning of some existing space-time coding schemes and a theoretical scheme based on Gaussian codes.

This paper has sparked a number of research activities to propose practical techniques approaching the optimal tradeoff. In [2], Yao and Wornell *et al* proposed a numerically optimized rotation based code that achieves the optimal tradeoff for a 2×2 channel. More recently, Tavildar and Viswanath [3] introduced a design criterion for permutation codes in order to achieve the diversity-vs-multiplexing optimal tradeoff for the parallel channel, that results from the Zero-Forcing equalized orginal MIMO channel. This equalization results in a degraded tradeoff when compared to the original channel. Furthermore, the permutation codes have to be optimized for every setting (constellation size and number of transmit antennas), which limits their application for rate adaptive systems.

Another technique, LAST, based on lattice coding was proposed by El Gamal *et al* in [4]. It achieves the optimal trade-off. In [4], it is stated that the use of LAST codes, as opposed to Linear Dispersion (LD) codes, is essential to attain the optimal tradeoff. However, the technique proposed in this paper is a special form of LD codes and the proposed technique also attains the optimal tradeoff. The essential difference between LAST and LD codes is one of shaping region, which is a hypersphere for LAST codes and a hypercube for LD codes. A hypersphere allows for some coding gain but is non-essential for the tradeoff considered here. On the other hand, the shaping region and dithering considered in [4] lead to a significant complexity increase in both transmitter and receiver. Furthermore, no explicit lattice construction is provided in [4]. And, if a lattice code can be found, it needs to be adapted for every (multiplexing) rate used. In LD codes, one only needs to adapt a simple symbol (e.g. QAM) constellation. With the use of a sphere decoder, the decoder complexity in [4] is cubic in T where $T \geq N_r + N_t - 1$. The use of the sphere decoder for the joint decoding in the DFE receiver proposed here would lead to a complexity that is cubic in N_t.

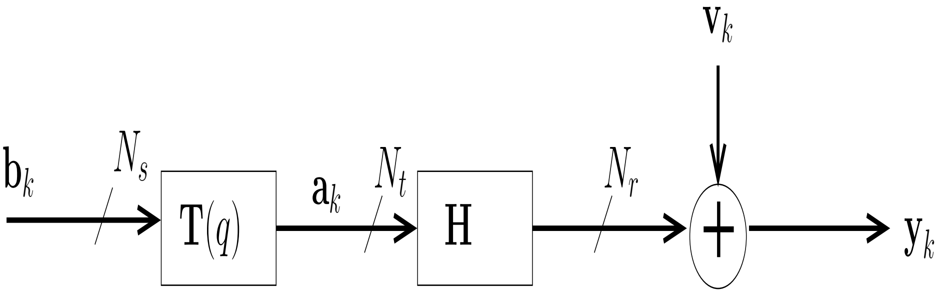

Fig. 1. MIMO transmission with Space-Time Spreading.

A. Space-Time Spreading (STS) Scheme

The $N_t \times N_r$ MIMO system with single-carrier transmission is shown in Fig. 1 and is essentially described by

$$\boldsymbol{y}_k = \mathbf{H}\,\boldsymbol{a}_k + \boldsymbol{v}_k = \mathbf{H}\,\mathbf{T}(q)\,\boldsymbol{b}_k + \boldsymbol{v}_k \tag{1}$$

where the white noise power spectral density matrix is $S_{\boldsymbol{vv}}(z) = \sigma_v^2\, I_{N_r}$, and $q^{-1}\,\boldsymbol{b}_k = \boldsymbol{b}_{k-1}$ denotes the one sample time delay operator. We consider the case of channel state information being absent at the transmitter (Tx) and perfect at the receiver (Rx). The channel elements are assumed to be i.i.d. Rayleigh fading. The linear precoding considered here (introduced in [5] and further analyzed in [6]) consists of a modification of VBLAST, obtained by inserting a square matrix prefilter $\mathbf{T}(z)$ before inputting the vector signal $\boldsymbol{b}_k$ into the channel $\mathbf{H}$. The $N_s = N_t$ ("full rate") component signals of $\boldsymbol{b}_k$ are called streams or layers. The suggested prefilter is

$$\begin{aligned} \mathbf{T}(z) &= \mathbf{D}(z)\,\mathbf{Q}\,, & |\mathbf{Q}_{ij}| &= \tfrac{1}{\sqrt{N_t}} \\ \mathbf{D}(z) &= \operatorname{diag}\{1,\, z^{-1}, \ldots, z^{-(N_t-1)}\}\,, & \mathbf{Q}^H\mathbf{Q} &= I \end{aligned} \tag{2}$$

with

$$\mathbf{Q} = \frac{1}{\sqrt{N_t}} \begin{bmatrix} 1 & \theta_1 & \ldots & {\theta_1}^{N_t-1} \\ 1 & \theta_2 & \ldots & {\theta_2}^{N_t-1} \\ \vdots & \vdots & & \vdots \\ 1 & \theta_{N_t} & \ldots & {\theta_{N_t}}^{N_t-1} \end{bmatrix}, \tag{3}$$

where the θ_i are the roots of $\theta^{N_t} - j = 0\,,\; j = \sqrt{-1}$.

Note that for a channel with a delay spread of L symbol periods, the prefilter can be immediately adapted by replacing the elementary delay z^{-1} by z^{-L} in $\mathbf{D}(z)$. In what follows, we focus on the frequency-flat channel case, in which case symbol stream m ($b_{m,k}$) passes through the equivalent SIMO channel $\sum_{i=1}^{N_t} z^{-(i-1)}\mathbf{H}_{:,i}\mathbf{Q}_{i,m}$ which now has memory due to the delay diversity introduced by $\mathbf{D}(z)$. It is important that the different columns $\mathbf{H}_{:,i}$ of the channel matrix get spread out in time to get full diversity (otherwise the streams just pass through a linear combination of the columns, as in VBLAST, which offers limited diversity). The delay diversity only becomes effective by the introduction of the spatial spreading matrix $\mathbf{Q}$, which has equal magnitude elements for uniform diversity spreading. The specific Vandermonde choice for $\mathbf{Q}$ shown in (3) corresponds to the DFT matrix multiplied by a diagonal matrix containing the elements of the first row of $\mathbf{Q}$. This choice for $\mathbf{Q}$ can be shown to lead to maximum coding gain in case of QAM symbols [5],[6]), among all matrices with normalized columns. With the proposed space-time spreading, each symbol stream has the same Matched Filter Bound (MFB), which is proportional to the channel Frobenius norm, namely $\text{MFB} = \rho\frac{1}{N_t}\,||\mathbf{H}||_F^2$. Hence full diversity (regardless of channel fading structure, and equal to N_tN_r for i.i.d. fading), is exploited. Also, since the prefilter $\mathbf{T}(z)$ is paraunitary and transforms the white vector stream $\boldsymbol{b}_k$ into the white vector stream $\boldsymbol{a}_k$, no loss in ergodic capacity is incurred. The STS scheme discussed here has been introduced in [5],[6]) as a full (symbol) rate full diversity scheme. With hindsight, such a scheme in signal processing parlance meant a scheme that can reach the endpoints on both axes of the optimal diversity-vs-multiplexing tradeoff curve. However, whether the whole optimal curve can be attained depends on the receiver, as illustrated in this paper with two examples.

A strongly related approach with an interesting interpretation is obtained as follows. Consider grouping the symbol sequence $\boldsymbol{b}_k$ in groups of N_t consecutive symbols, then one group $\boldsymbol{b}_{k-N_t+1:k}$ of N_t symbols forms a square matrix of size $N_t \times N_t$. An alternative approach is obtained by transposing the matrix $\boldsymbol{b}_{k-N_t+1:k}$ before inputting its colums into $\mathbf{T}(z)$ (hence inputting the rows of $\boldsymbol{b}_{k-N_t+1:k}$ into $\mathbf{T}(z)$ instead of the columns, this interleaving has no effect if no channel coding is introduced). It corresponds to spreading within streams instead of between streams. The resulting scheme can be interpreted as follows. It corresponds to the sawtooth threading approach of [7], which transforms the time-invariant (flat) MIMO channel into a periodically time-varying SIMO channel for each stream (period N_t), and then the temporal fading gets exploited with the

$N_t \times N_t$ constellation rotation matrix $\mathbf{Q}$ as suggested in [8].

In the case of linear dispersion codes [9],[10], a packet of T vector symbols $\boldsymbol{a}_k$ (hence a $N_t \times T$ matrix) gets constructed as a linear combination of fixed matrices in which the combination coefficients are symbols b_k. A particular case is the Alamouti code which is a full diversity single rate code corresponding to block length $T = N_t = 2$, $N_s = 1$. Here we focus on essentially continuous transmission in which linear precoding corresponds to MIMO prefiltering. The *linear convolutive precoding* scheme proposed here can also be considered as a special case of linear dispersion codes (making abstraction of the packet boundaries) in which the fixed matrices are time-shifted versions of the impulse responses of the columns of the MIMO prefilter $\mathbf{T}(z)$.

In what follows we denote the overall channel by $\mathbf{G}(z) \triangleq \mathbf{HT}(z)$. At the receiver side we propose a decision feedback equalizer (DFE) receiver. This receiver, as we will see, achieves the optimal diversity versus multiplexing trade-off and has an acceptable complexity that results from a sphere decoding of a vector of size N_t. The drawback of the DFE receiver is the error propagation due to the successive detection and cancellation. The error propagation has no impact on the frame error rate, but it degrades the symbol (and bit) error rate. To avoid this, we can take advantage of the presence of binary channel codes (used in general for error correction) and choose appropriate codes, like those introduced in [11], [12], that allow successive joint detection and decoding.

B. Frame Structure

Although the proposed linear prefiltering technique is ideally intended for continuous transmission, in practice data gets transmitted in packets or frames. As with convolutional channel codes, the proposed convolutive linear precoding may require proper handling of the frame borders. The memory introduced by the prefiltering does not have to lead to interframe interference, at least for a frequency-flat channel, if circulant convolution would be used for the prefilter. However, the requirement of proper initialization of a Decision Feedback Equalizer (DFE), as proposed here, necessitates the introduction of a guard interval of size equal to the memory of the DFE feedback filter, which is equal to the size of the memory of the prefilter, hence of size $N_t{-}1$ symbol periods. We shall assume w.l.o.g. that the frame of T symbol periods starts with a guard interval of size $N_t{-}1$ followed by data symbols at time $k = 1, 2, \ldots, T{-}N_t{+}1$, and is followed by the guard interval of the next frame. The introduction of the guard interval leads to a reduction in rate by a factor $1 - \frac{N_t - 1}{T}$ which can be made arbitrarily small by increasing the frame length T. We shall neglect this reduction in the sequel to simplify notation.

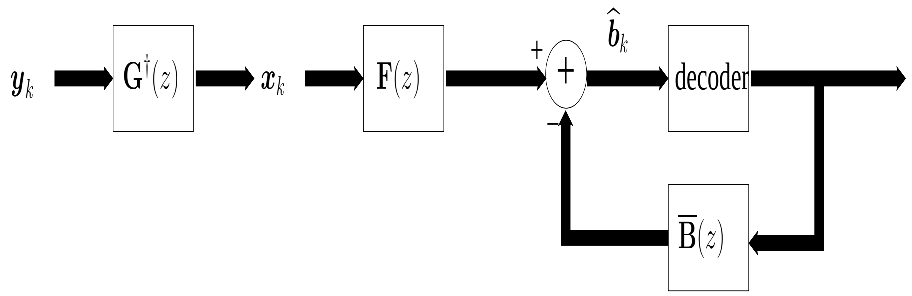

Fig. 2. Conventional MIMO DFE receiver.

II. Conventional MIMO DFE Receiver

Consider the classical MIMO DFE, in which the symbol vectors $\boldsymbol{b}_k$ are processed sequentially in time (see Fig. 2). We call this the conventional MIMO DFE [13], as opposed to the sequential processing MIMO DFE (an extension of the VBLAST Rx to channels with memory) in which the component sequences of $\boldsymbol{b}_k$ are processed sequentially (in component order) [14].

The Rx starts with a preprocessing by the matched filter (MF) $\mathbf{G}^{\dagger}(z)$, the output of which is $\boldsymbol{x}_k = \mathbf{G}^{\dagger}(q)\,\boldsymbol{y}_k$. The DFE, operating on the MF output, produces the following symbol estimate

$$\widehat{\boldsymbol{b}}_k \;=\; -\underbrace{\overline{\mathbf{B}}(q)}_{\text{feedback}}\;\boldsymbol{b}_k + \underbrace{\mathbf{F}(q)}_{\text{feedforward}}\;\boldsymbol{x}_k\,, \tag{4}$$

where the feedback filter $\overline{\mathbf{B}}(z) = \sum_{i=1}^{N_t-1} \mathbf{B}_i z^{-i}$ is such that $\mathbf{B}(z) = I_{N_t} + \overline{\mathbf{B}}(z)$ is causal, monic and minimum phase. There are two possible designs of interest for the DFE filters, the Minimum Mean Squared Error (MMSE) and the MMSE Zero Forcing (ZF) designs. We consider the MMSE design first.

A. MMSE Conventional MIMO DFE Rx

The linear MMSE symbol vector estimate (MMSE linear equalizer output) can be expressed as

$$\begin{aligned}\widehat{\boldsymbol{b}}_k^{lmmse} &= \mathbf{S}_{\boldsymbol{by}}(q)\,\mathbf{S}_{\boldsymbol{yy}}^{-1}(q)\,\boldsymbol{y}_k \;=\; \sigma_a^2\mathbf{G}^{\dagger}(q)(\sigma_a^2\mathbf{G}(q)\mathbf{G}^{\dagger}(q)+\sigma_v^2\mathbf{I})^{-1}\,\boldsymbol{y}_k \\ &= (\mathbf{G}^{\dagger}(q)\mathbf{G}(q)+\tfrac{1}{\rho}\mathbf{I})^{-1}\,\mathbf{G}^{\dagger}(q)\,\boldsymbol{y}_k \;=\; \mathbf{R}^{-1}(q)\,\boldsymbol{x}_k\end{aligned} \tag{5}$$

where $\mathbf{R}(z) = \mathbf{G}^{\dagger}(z)\mathbf{G}(z) + \frac{1}{\rho}I$ and $\rho = \frac{\sigma_a^2}{\sigma_v^2}$. The symbol estimate leads to symbol estimation error $\widetilde{\boldsymbol{b}}_k^{lmmse} = \boldsymbol{b}_k - \widehat{\boldsymbol{b}}_k^{lmmse}$ and we can write

$$\boldsymbol{b}_k \;=\; \widehat{\boldsymbol{b}}_k^{lmmse} + \widetilde{\boldsymbol{b}}_k^{lmmse} \;=\; \mathbf{R}^{-1}(q)\,\boldsymbol{x}_k + \widetilde{\boldsymbol{b}}_k^{lmmse}\,. \tag{6}$$

The orthogonality principle of MMSE estimation leads to the power spectral density matrix

$$\mathbf{S}^{lmmse}_{\widetilde{\boldsymbol{b}}\widetilde{\boldsymbol{b}}}(z) = \mathbf{S}_{\boldsymbol{b}\boldsymbol{b}}(z) - \mathbf{S}^{lmmse}_{\widehat{\boldsymbol{b}}\widehat{\boldsymbol{b}}}(z) = \sigma_v^2\,\mathbf{R}^{-1}(z)\,. \tag{7}$$

Consider now the minimum and maximum phase spectral factorization of $\mathbf{R}(z)$ (see [13]). Let $\mathbf{B}(z)$ be the unique causal, monic ($\mathbf{B}(\infty) = I_{N_t}$) minimum phase factor of $\mathbf{R}(z)$, then

$$\mathbf{R}(z) \;=\; \mathbf{B}^{\dagger}(z)\,\mathbf{M}\,\mathbf{B}(z). \tag{8}$$

where $\mathbf{M}$ is a constant positive definite hermitian matrix. Then $\widehat{\boldsymbol{b}}_k^{lmmse} = \mathbf{B}^{-1}(q)\,\mathbf{M}^{-1}\,\mathbf{B}^{-\dagger}(q)\,\boldsymbol{x}_k$. By canceling the anticausal InterSymbol Interference (ISI) linearly, namely by choosing $\mathbf{F}(q) = \mathbf{M}^{-1}\mathbf{B}^{-\dagger}(q)$, we get the DFE Rx

$$\begin{aligned}\mathbf{F}(q)\,\boldsymbol{x}_k &= \mathbf{M}^{-1}\,\mathbf{B}^{-\dagger}(q)\,\boldsymbol{x}_k \;=\; \mathbf{M}^{-1}\,\mathbf{B}^{-\dagger}(q)\,\mathbf{R}(q)\,(\boldsymbol{b}_k - \widetilde{\boldsymbol{b}}_k^{lmmse})\\ &= \mathbf{B}(q)\,\boldsymbol{b}_k + \mathbf{B}(q)\,\widetilde{\boldsymbol{b}}_k^{lmmse} \;=\; \mathbf{B}(q)\,\boldsymbol{b}_k + \boldsymbol{e}_k \;=\; \boldsymbol{b}_k + \overline{\mathbf{B}}(q)\,\boldsymbol{b}_k + \boldsymbol{e}_k\,,\end{aligned} \tag{9}$$

and hence

$$\widehat{\boldsymbol{b}}_k^{mmsedfe} = \mathbf{F}(q)\,\boldsymbol{x}_k - \overline{\mathbf{B}}(q)\,\boldsymbol{b}_k = \boldsymbol{b}_k + \boldsymbol{e}_k \tag{10}$$

and in fact $\boldsymbol{e}_k = -\widetilde{\boldsymbol{b}}_k^{mmsedfe}$ with $\mathbf{S}_{\boldsymbol{e}\boldsymbol{e}}(z) = \sigma_v^2\,\mathbf{B}(z)\mathbf{R}^{-1}(z)\mathbf{B}^{\dagger}(z) = \sigma_v^2\,\mathbf{M}^{-1}$ (hence $\boldsymbol{e}_k$ is temporally white). The feedback filter $\overline{\mathbf{B}}(z) = \mathbf{B}(z) - I$ is closely related to the backward MIMO prediction error filter $\mathbf{P}^{\dagger}(z)$ of the spectrum $\mathbf{R}(z)$, which satisfies $\mathbf{P}^{\dagger}(z)\mathbf{R}(z)\mathbf{P}(z) =$ Constant Matrix. Indeed, obviously $\mathbf{P}(z) = \mathbf{B}^{-1}(z)$ and Constant Matrix $= M$. So M is the covariance matrix of the backward prediction error vector of the spectrum $\mathbf{R}(z)$. The following Theorem provides $\mathbf{B}(z)$ in the case of a frequency flat MIMO channel.

Theorem 1: *For a frequency-flat MIMO channel combined with the proposed precoder filter $\mathbf{T}(z)$ in (2), the feedback filter is*

$$\mathbf{B}(z) = \mathbf{T}^{\dagger}(z)\,\mathbf{L}^{H}\,\mathbf{T}(z)\,, \tag{11}$$

with corresponding

$$\mathbf{M} = \mathbf{Q}^{H}\Sigma\mathbf{Q}\,, \tag{12}$$

where $\mathbf{L}$ and Σ result from the LDU triangular matrix factorization of $\mathbf{H}^H\mathbf{H} + \frac{1}{\rho}I = \mathbf{L}\,\Sigma\,\mathbf{L}^H$.

Let $\Sigma = \operatorname{diag}\{\sigma_1, \ldots, \sigma_{N_t}\}$ and note that (12) corresponds to the eigendecomposition of M.

Proof : We need to show that $\mathbf{B}(z) = \mathbf{T}^{\dagger}(z)\,\mathbf{L}^{H}\,\mathbf{T}(z) = \mathbf{Q}^{H}\,\mathbf{D}^{\dagger}(z)\,\mathbf{L}^{H}\,\mathbf{D}(z)\,\mathbf{Q}$ is a minimum phase causal monic filter and verifies $\mathbf{B}^{-\dagger}(z)\mathbf{R}(z)\mathbf{B}^{-1}(z) =$ Constant Matrix. Since $\mathbf{L}^H$ is upper triangular with unit diagonal, then due to the diagonal structure of $\mathbf{D}(z)$, $\mathbf{D}^{\dagger}(z)\,\mathbf{L}^{H}\,\mathbf{D}(z)$ is a monic causal filter. As $\mathbf{Q}$ is unitary, $\mathbf{B}(z)$ is also a causal monic filter. Furthermore $\det\mathbf{B}(z) = \det\mathbf{L}^{H} = 1$, which shows that $\mathbf{B}(z)$ is minimum phase. To complete the proof of the theorem it is sufficient to verify that $\mathbf{B}^{-\dagger}(z)\,\mathbf{R}(z)\,\mathbf{B}^{-1}(z) = \mathbf{Q}^{H}\,\Sigma\,\mathbf{Q} = \mathbf{M}$ is a constant matrix. □

Unbiased MMSE (UMMSE) Conventional MIMO DFE Rx

The discussion below will be valid also for the case $N_t > N_r$. This will lead to singular matrices and requires the introduction of (Moore-Penrose) pseudoinverses [15] which will be denoted by $(.)^{\sharp}$. Now, it is well-known that $\widehat{\boldsymbol{b}}_k^{mmsedfe} = \mathbf{F}(q)\,\boldsymbol{x}_k - \overline{\mathbf{B}}(z)\,\boldsymbol{b}_k$ is a biased estimate of $\boldsymbol{b}_k$, since indeed

$$\begin{aligned}
\mathbf{F}(q)\,\boldsymbol{x}_k - \overline{\mathbf{B}}(q)\,\boldsymbol{b}_k &= [\mathbf{M}^{-1}\,\boldsymbol{b}^{-\dagger}(q)\,\mathbf{G}^{\dagger}(q)\mathbf{G}(q) - \overline{\mathbf{B}}(z)]\,\boldsymbol{b}_k + \mathbf{M}^{-1}\,\mathbf{B}^{-\dagger}(q)\mathbf{G}^{\dagger}(q)\,\boldsymbol{v}_k \\
&= (I - \tfrac{1}{\rho}\,\mathbf{M}^{-1}\,\mathbf{B}^{-\dagger}(q))\,\boldsymbol{b}_k + \mathbf{M}^{-1}\,\mathbf{B}^{-\dagger}(q)\mathbf{G}^{\dagger}(q)\,\boldsymbol{v}_k \\
&= (I - \tfrac{1}{\rho}\,\mathbf{M}^{-1})\,\boldsymbol{b}_k + \widetilde{\boldsymbol{e}}_k\,,
\end{aligned} \tag{13}$$

where the sample

$$\widetilde{\boldsymbol{e}}_k = \mathbf{M}^{-1}\,\boldsymbol{b}^{-\dagger}(q)\mathbf{G}^{\dagger}(q)\,\boldsymbol{v}_k - \frac{1}{\rho}\,\mathbf{M}^{-1}\,(\boldsymbol{b}^{-\dagger}(q) - I)\,\boldsymbol{b}_k \tag{14}$$

is now uncorrelated with the sample b_k. The covariance matrix of the vector $\widetilde{\boldsymbol{e}}_k$ is

$$\begin{aligned}
\mathbf{C}_{\widetilde{\boldsymbol{e}}\widetilde{\boldsymbol{e}}} &= \oint \tfrac{dz}{j2\pi\,z}\,[\mathbf{M}^{-1}(\sigma_v^2\,\mathbf{B}^{-\dagger}(z)\mathbf{G}^{\dagger}(z)\mathbf{G}(z)\mathbf{B}(z) + \sigma_b^2\,\rho^{-2}(\mathbf{B}^{-\dagger}(z) - I)(\mathbf{B}^{-1}(z) - \mathbf{I}))\,\mathbf{M}^{-1}] \\
&= \oint \tfrac{dz}{j2\pi\,z}\,[\mathbf{M}^{-1}(\sigma_v^2\mathbf{B}^{-\dagger}(z)\mathbf{G}^{\dagger}(z)\mathbf{G}(z)\mathbf{B}(z) + \sigma_v^2\,\rho^{-1}\mathbf{B}^{-\dagger}(z)\mathbf{B}^{-1}(z))\mathbf{M}^{-1}] - \sigma_v^2\rho^{-1}\mathbf{M}^{-2} \\
&= \oint \tfrac{dz}{j2\pi\,z}\,\mathbf{M}^{-1}(\sigma_v^2\mathbf{B}^{-\dagger}(z)(\mathbf{G}^{\dagger}(z)\mathbf{G}(z) + \rho^{-1}\mathbf{I})\mathbf{B}^{-1}(z))\mathbf{M}^{-1} - \sigma_v^2\,\rho^{-1}\mathbf{M}^{-2} \\
&= \oint \tfrac{dz}{j2\pi\,z}\,(\mathbf{M}^{-1}\sigma_v^2\mathbf{M}\mathbf{M}^{-1}) - \sigma_v^2\,\rho^{-1}\mathbf{M}^{-2} \\
&= \sigma_v^2\,\mathbf{M}^{-1}(I - \tfrac{1}{\rho}\,\mathbf{M}^{-1})\,.
\end{aligned} \tag{15}$$

The UMMSE feedforward filter is

$$\mathbf{F}^{U}(q) = (I - \frac{1}{\rho}\,\mathbf{M}^{-1})^{\sharp}\,\mathbf{M}^{-1}\mathbf{B}^{-\dagger}(q) = (\mathbf{M} - \frac{1}{\rho}\,I)^{\sharp}\,\mathbf{B}^{-\dagger}(q), \tag{16}$$

whereas the corresponding feedback filter is

$$\overline{\mathbf{B}}^{U}(q) = (I - \frac{1}{\rho}\,\mathbf{M}^{-1})^{\sharp}\,(\mathbf{B}(q) - I)\,. \tag{17}$$

The output of the DFE is then

$$\begin{aligned}
\widehat{\boldsymbol{b}}_k^{U} &= \mathbf{F}^{U}(q)\,\boldsymbol{x}_k - \overline{\mathbf{B}}^{U}(q)\,\boldsymbol{b}_k \\
&= \boldsymbol{b}_k + \tilde{\boldsymbol{e}}_k^{U}\,,
\end{aligned} \tag{18}$$

where $\mathbf{C}_{\widetilde{\boldsymbol{e}}^U \widetilde{\boldsymbol{e}}^U} = \sigma_v^2 \mathbf{M}^{-1}(I - \frac{1}{\rho}\mathbf{M}^{-1})^{\sharp}$. The capacity[1] of such a Tx system with UMMSE DFE Rx, assuming perfect feedback and joint decoding of the components of $\boldsymbol{b}_k$, is (interpreting (18) as a vector AWGN channel)

$$\begin{aligned} C &= \ln\det(\mathbf{I} + \sigma_a^2 \mathbf{C}^{\sharp}_{\widetilde{\boldsymbol{e}}^U \widetilde{\boldsymbol{e}}^U}) \\ &= \ln\det(\mathbf{I} + \rho(I - \tfrac{1}{\rho}\mathbf{M}^{-1})\mathbf{M}) \\ &= \ln\det(\rho\,\mathbf{M})\,. \end{aligned} \tag{19}$$

In order to show that C equals the capacity of the MIMO channel, note that

$$\begin{aligned} C &= \ln\det(\rho\,\mathbf{M}) \;=\; \ln\det(\rho\,\Sigma) \;=\; \ln\det(I_{N_t} + \rho\,\mathbf{H}^H\,\mathbf{H}) \\ &= \ln\det(I_{N_r} + \rho\,\mathbf{H}\,\mathbf{H}^H) \;=\; \oint \tfrac{dz}{j2\pi\, z} \ln\det(I_{N_r} + \rho\,\mathbf{G}(z)\,\mathbf{G}^{\dagger}(z)) \end{aligned} \tag{20}$$

since $\det(\mathbf{Q}^H\,\mathbf{Q}) = 1$ and $\det(\mathbf{L}) = 1$. Hence such a Rx and decoding strategy conserves capacity. The linear precoding introduces memory into the equivalent channel $\mathbf{G}(z)$, whereas the DFE makes the equivalent channel memoryless again (temporal correlation in the noise gets ignored at the DFE detection point).

B. MMSE ZF Conventional MIMO DFE Rx

For this case we need to assume $N_r \geq N_t$. The linear MMSE Zero Forcing (ZF) symbol vector estimate is

$$\begin{aligned} \widehat{\boldsymbol{b}}_k^{lmmse\,zf} &= (\mathbf{G}^{\dagger}(q)\mathbf{G}(q))^{-1}\mathbf{G}^{\dagger}(q)\,\boldsymbol{y}_k \\ &= \mathbf{R}^{-1}(q)\,\boldsymbol{x}_k \end{aligned} \tag{21}$$

where now $\mathbf{R}(z) = \mathbf{G}^{\dagger}(z)\mathbf{G}(z)$. Consider again the spectral factorization $\mathbf{R}(z) = \mathbf{B}^{\dagger}(z)\,\mathbf{M}\,\mathbf{B}(z)$. Then in the same way as for the MMSE design, and again with the usual DFE analysis assumption that detected symbols (in the feedback) are correct, we get

$$\begin{aligned} \widehat{\boldsymbol{b}}_k^{mmzfdfe} &= \mathbf{F}(q)\,\boldsymbol{x}_k - \overline{\mathbf{B}}(q)\,\boldsymbol{b}_k \\ &= \boldsymbol{b}_k + \boldsymbol{e}_k\,, \end{aligned} \tag{22}$$

where $\mathbf{F}(q) = \mathbf{M}^{-1}\mathbf{B}^{-\dagger}(q)$, $\mathbf{B}(q) = \mathbf{T}^{\dagger}(q)\,\mathbf{L}^H\,\mathbf{T}(q)$, $\mathbf{S}_{\boldsymbol{e}\boldsymbol{e}}(z) = \sigma_v^2\,\mathbf{M}^{-1}$, $\mathbf{M} = \mathbf{Q}^H\mathbf{D}\mathbf{Q}$, and this time $\mathbf{L}$, $\mathbf{D}$ result from the LDU factorization of $\mathbf{H}^H\mathbf{H} = \mathbf{L}\,\mathbf{D}\,\mathbf{L}^H$. Unlike the MMSE design, the MMSE ZF design makes no compromise between noise enhancement and interference cancellation. It removes (zero-forces) the entire interference. Hence bias is not an issue and the noise at the output of the equalizer, $\boldsymbol{e}_k$, is Gaussian.

[1]The notion of capacity will be used loosely here, in the sense of mutual information for the case of Gaussian inputs with the same spectrum.

In both DFE designs, the feedback filter $\mathbf{B}(z)$ is monic causal and FIR of length N_t, and by the same analysis the feedforward filter $\mathbf{F}(z) = \mathbf{M}^{-1}\mathbf{Q}^H\mathbf{D}^{\dagger}(z)\,\mathbf{L}^{-1}\,\mathbf{D}(z)\,\mathbf{Q}$ is anticausal and FIR of length N_t also. Note that $\mathbf{B}^{-1}(z)$ is FIR because $\mathbf{B}(z)$ does not have zeros. In both DFE designs, different choices are possible for the detection of the symbol vector $\boldsymbol{b}_k$. For example a V-BLAST-like detector can be used. However, such a sequential processing of the symbol vector components degrades performance. The optimal choice is the joint detection of the components of $\boldsymbol{b}_k$ using a weighted minimum distance detector which in the MMSE ZF case minimizes $||\widehat{\boldsymbol{b}}_k - \boldsymbol{b}_k||^2_{\mathbf{C}^{-1}_{\boldsymbol{ee}}} = (\widehat{\boldsymbol{b}}_k - \boldsymbol{b}_k)^H\mathbf{C}^{-1}_{\boldsymbol{ee}}(\widehat{\boldsymbol{b}}_k - \boldsymbol{b}_k)$ w.r.t. $\boldsymbol{b}_k$ ($\widehat{\boldsymbol{b}}_k$ is the DFE output). Such a detector has an acceptable complexity especially for a small number of transmit antennas and small constellation size. The complexity can be reduced by the use of sphere decoding. Such a DFE detector with joint decoding is less complex than direct Maximum Likelihood Sequence Estimation (MLSE), which could in principle be done with the Viterbi algorithm, but in which the number of states grows exponentially with N_t^2 (instead of N_t for joint detection in the DFE) due to the memory of $N_t{-}1$ introduced by the precoder $\mathbf{T}(z)$.

III. Diversity-vs-Multiplexing Tradeoff

In what follows, we study the diversity-vs-multiplexing tradeoff achieved by the Conventional MIMO DFE equalizer, applied to the linearly precoded system considered here.

A. Case of UMMSE DFE Design

Theorem 2: *In the case of a frequency-flat channel, $N_t = 2^n$ (n integer), the use of a weighted minimum distance detector and QAM constellations allows the Conventional MIMO DFE Rx, with* **UMMSE design***, to achieve the optimal diversity-vs-multiplexing tradeoff given by $d^*(r)$ (see [1]). $d^*(r)$ is given by the piecewise-linear function connecting the points $(k, d^*(k))$, $k = 0, 1, \ldots, p$, where*

$$d^*(k) = (p-k)(q-k) \tag{23}$$

with $p = \min\{N_r, N_t\}$ and $q = \max\{N_r, N_t\}$.

This theorem shows that the proposed transmitter-receiver combination with UMMSE design allows to attain the optimal diversity-vs-multiplexing tradeoff derived in [1].

Proof : Consider the unbiased MMSE Conventional MIMO DFE Rx. Let $\doteq$ denote exponential equality, *i.e.*, $f(\rho) \doteq \rho^b$ means

$$\lim_{\rho\to\infty} \frac{\ln f(\rho)}{\ln(\rho)} = b\,. \tag{24}$$

The proof of Theorem 2 is structured in three steps. In Step 1 we characterize the frame (block) error probability in terms of the probability of a first symbol error. In Step 2 we derive a lower bound on this first symbol error probability. Finally, in Step 3, we characterize the behavior of the error probability for large SNR and derive the diversity-vs-multiplexing tradeoff.

Step 1:

The symbol vectors of the transmitted frame are detected sequentially in time using the DFE Rx. We denote by E_k the event of making an error when detecting the k^{th} symbol vector $\boldsymbol{b}_k$ (E_k^c is the complement or the event in which no error is made when detecting the k^{th} symbol vector). Whenever there is an error on any of the detected symbols, the frame is said to be in error. P_e denotes the frame error probability. P_e is the probability of the union of individual error events E_k, $k = 1, \ldots, T-N_t+1$,

$$P_e = P(\cup_{k=1}^{T-N_t+1} E_k) \ . \tag{25}$$

The union and intersection of events is distributive, so the event $E_1 \cup E_2$ can be written as the union of the two events E_1 and $E_2 \cap E_1^c$,

$$E_1 \cup E_2 = E_1 \cup (E_2 \cap E_1^c) \ . \tag{26}$$

E_1 and $E_2 \cap E_1^c$ are two disjoint sets ($E_1 \cap (E_2 \cap E_1^c) = \emptyset$), hence

$$P(E_1 \cup E_2) = P(E_1) + P(E_2, E_1^c), \tag{27}$$

where $P(A, B)$ denotes $P(A \cap B)$. Exploiting this fact, we can show by recursion that

$$P_e = \sum_{k=1}^{T-N_t+1} P(E_k, E_1^c, E_2^c, \ldots, E_{k-1}^c) \tag{28}$$

Since probability is non-negative, $P_e \geq P(E_1)$, and obviously $P_e \dot{\geq} P(E_1)$. We would like to show that $P_e \doteq P(E_1)$, which will be obtained if we can show that $P_e \dot{\leq} P(E_1)$. Since T is finite, it is sufficient to show that $P(E_k, E_1^c, E_2^c, \ldots, E_{k-1}^c) \dot{\leq} P(E_1)$ for any $k \in \{2, \ldots, T-N_t+1\}$. To that end, consider a genie-aided receiver that has access to the correct value of the past detected symbols $\boldsymbol{b}_i$, $i = 1, \ldots, k-1$ and cancels exactly the interference coming from these symbols. The genie-aided receiver reproduces for most of the frame the same situation of the first symbol for which there is no interference from the past. Then the probability of error of the genie-aided receiver when detecting symbol k, $P_k^{g.a} = P(E_k|\boldsymbol{b}_1,\ldots,\boldsymbol{b}_{k-1})$, satisfies

$$P_k^{g.a} \begin{cases} = & P(E_1) \quad , \; k=1,\ldots,T{-}2(N_t{-}1) \\ \le & P(E_1) \quad , \; k=T{-}2N_t{+}3,\ldots,T{-}N_t{+}1\,. \end{cases} \tag{29}$$

Indeed, the DFE symbol estimation error is stationary as far as the noise contribution is concerned, whereas for the residual ISI, it is determined by the filter $\mathbf{F}(z)\mathbf{G}^\dagger(z)\,\mathbf{G}(z) - \mathbf{B}(z) = -\frac{1}{\rho}\,\mathbf{F}(z)$ which is anticausal and FIR of memory $N_t{-}1$. So the ISI is stationary for most of the frame, except for the last $N_t{-}1$ symbols, where less future symbols interfere due to the following guard interval. The second part of (29) will be discussed at the end of Step 2. On the other hand

$$\begin{aligned} P_k^{g.a} &= P(E_k|\boldsymbol{b}_1,\ldots,\boldsymbol{b}_{k-1}) \\ &\ge P(E_k,(E_1^c,E_2^c,\ldots,E_{k-1}^c)|\boldsymbol{b}_1,\ldots,\boldsymbol{b}_{k-1}) \\ &= P(E_k|E_1^c,E_2^c,\ldots,E_{k-1}^c,\boldsymbol{b}_1,\ldots,\boldsymbol{b}_{k-1})\,P(E_1^c,E_2^c,\ldots,E_{k-1}^c|\boldsymbol{b}_1,\ldots,\boldsymbol{b}_{k-1})\,. \end{aligned} \tag{30}$$

In the event $(E_1^c,E_2^c,\ldots,E_{k-1}^c)$, the symbols $\boldsymbol{b}_1,\ldots,\boldsymbol{b}_{k-1}$, are correctly detected, which provides access to their true values, hence

$$P(E_k|E_1^c,E_2^c,\ldots,E_{k-1}^c,\boldsymbol{b}_1,\ldots,\boldsymbol{b}_{k-1}) = P(E_k|E_1^c,E_2^c,\ldots,E_{k-1}^c). \tag{31}$$

Obviously, when knowing the true values of $\boldsymbol{b}_1,\ldots,\boldsymbol{b}_{k-1}$, the probability to make an error on deciding them is zero, hence

$$P(E_1^c,E_2^c,\ldots,E_{k-1}^c|\boldsymbol{b}_1,\ldots,\boldsymbol{b}_{k-1}) = 1\,, \tag{32}$$

and (30) becomes

$$\begin{aligned} P_k^{g.a} &\ge P(E_k|E_1^c,E_2^c,\ldots,E_{k-1}^c) \\ &\ge P(E_k|E_1^c,E_2^c,\ldots,E_{k-1}^c)P(E_1^c,E_2^c,\ldots,E_{k-1}^c) \\ &= P(E_k,E_1^c,E_2^c,\ldots,E_{k-1}^c), \end{aligned} \tag{33}$$

where in the second inequality we used the fact that $P(E_1^c,E_2^c,\ldots,E_{k-1}^c) \le 1$. Combining (29) and (33), we conclude that $P(E_k,E_1^c,E_2^c,\ldots,E_{k-1}^c) \le P(E_1)$, and from (28)

$$P_e \le (T - N_t + 1)P(E_1)\,. \tag{34}$$

Since T is finite, $P_e \dot{\le} P(E_1)$. The desired result then follows

$$P_e \doteq P(E_1). \tag{35}$$

The above results are independent of the criterion used for the design of the equalizer filters, and assume only the DFE structure.

Step 2:

In this step of the proof, we derive a lower bound on the first symbol error probability for a fixed channel realization $P(E_1|\mathbf{H})$. In Step 2, we shall denote $\boldsymbol{b}_1$ as $\boldsymbol{b}$ to simplify notation. We use the weighted minimum distance detector at the output of the UMMSE Conventional MIMO DFE (18):

$$||\widehat{\boldsymbol{b}}^U - \boldsymbol{b}'||^2_{\mathbf{C}^\sharp_{\widetilde{\boldsymbol{e}}^U\widetilde{\boldsymbol{e}}^U}} = ||\widehat{\boldsymbol{b}} - (I - \frac{1}{\rho}\mathbf{M}^{-1})\boldsymbol{b}'||^2_{\mathbf{C}^\sharp_{\tilde{\boldsymbol{e}}\tilde{\boldsymbol{e}}}} \, . \tag{36}$$

An error occurs if we decide $\boldsymbol{b}' \neq \boldsymbol{b}$ for transmitted $\boldsymbol{b}$. For an error to occur we need to have

$$||\widehat{\boldsymbol{b}} - (I - \frac{1}{\rho}\mathbf{M}^{-1})\boldsymbol{b}'||^2_{\mathbf{C}^\sharp_{\tilde{\boldsymbol{e}}\tilde{\boldsymbol{e}}}} \leq ||\widehat{\boldsymbol{b}} - (I - \frac{1}{\rho}\mathbf{M}^{-1})\boldsymbol{b}||^2_{\mathbf{C}^\sharp_{\tilde{\boldsymbol{e}}\tilde{\boldsymbol{e}}}} \, , \tag{37}$$

where $\mathbf{C}_{\widetilde{\boldsymbol{e}}\widetilde{\boldsymbol{e}}} = \sigma_v^2\,\mathbf{M}^{-1}(I - \frac{1}{\rho}\mathbf{M}^{-1})$. If we denote by $\Delta\boldsymbol{b} = \boldsymbol{b} - \boldsymbol{b}'$, then (37) is equivalent to

$$\Delta\boldsymbol{b}^H(\mathbf{I} - \frac{1}{\rho}\mathbf{M}^{-1})\mathbf{C}^\sharp_{\tilde{\boldsymbol{e}}\tilde{\boldsymbol{e}}}(I - \frac{1}{\rho}\mathbf{M}^{-1})\Delta\boldsymbol{b} \;\leq\; 2\,\Re\{\Delta\boldsymbol{b}^H(\mathbf{I} - \frac{1}{\rho}\mathbf{M}^{-1})\mathbf{C}^\sharp_{\tilde{\boldsymbol{e}}\tilde{\boldsymbol{e}}}\,\widetilde{\boldsymbol{e}}\}, \tag{38}$$

where $\widetilde{\boldsymbol{e}} = \widetilde{\boldsymbol{e}}_1$ is defined in (14) and $\Re\{.\}$ denotes the real part of its argument. Consider now the rotated symbols $\boldsymbol{c} = \mathbf{Q}\,\boldsymbol{b}$. Then the MMSE DFE estimate $\widehat{\boldsymbol{c}} = \mathbf{Q}\,\widehat{\boldsymbol{b}}$ gets produced with the filters

$$\begin{aligned} \mathbf{B}_c(z) &= \mathbf{Q}\,\mathbf{B}(z)\,\mathbf{Q}^H \;=\; \mathbf{D}^\dagger(z)\,\mathbf{L}^H\,\mathbf{D}(z) \\ \mathbf{F}_c(z) &= \mathbf{Q}\,\mathbf{F}(z) \;=\; \Sigma^{-1}\,\mathbf{B}_c^{-1}(z)\,\mathbf{Q}\,. \end{aligned} \tag{39}$$

and the corresponding symbol estimation error $\mathbf{Q}\,\widetilde{\boldsymbol{e}}$ has a diagonal covariance matrix $\sigma_v^2\,\Sigma^{-1}(I - \frac{1}{\rho}\Sigma^{-1})$. Let $\Delta\boldsymbol{c} = \mathbf{Q}\Delta\boldsymbol{b}$ and $\widetilde{\boldsymbol{v}} = \mathbf{C}^{\sharp/2}_{\tilde{\boldsymbol{e}}\tilde{\boldsymbol{e}}}\widetilde{\boldsymbol{e}} = \sigma_v^{-1}\Sigma^{1/2}(\mathbf{I} - \frac{1}{\rho}\Sigma^{-1})^{\sharp/2}\mathbf{Q}\,\widetilde{\boldsymbol{e}}$. Note that $\mathbf{C}_{\widetilde{\boldsymbol{v}}\widetilde{\boldsymbol{v}}} = \mathbf{P}_{(I-\frac{1}{\rho}\Sigma^{-1})}$ which is the projection matrix on the column space of $(I - \frac{1}{\rho}\Sigma^{-1})$. $\mathbf{C}_{\widetilde{\boldsymbol{v}}\widetilde{\boldsymbol{v}}}$ is a diagonal matrix of ones and zeros, and hence verifies $\mathbf{C}_{\widetilde{\boldsymbol{v}}\widetilde{\boldsymbol{v}}} \leq \mathbf{I}_{N_t}$. Now, (38) translates to the following inequality for $\Delta\boldsymbol{c}$

$$\begin{aligned} \Delta\boldsymbol{c}^H\,\Sigma(I - \tfrac{1}{\rho}\,\Sigma^{-1})\,\Delta\boldsymbol{c} \;&\leq\; 2\sigma_v\,\Re\{\Delta\boldsymbol{c}^H(\mathbf{I} - \tfrac{1}{\rho}\Sigma^{-1})^{1/2}\Sigma^{1/2}\,\widetilde{\boldsymbol{v}}\} \\ &\leq\; 2\sigma_v\,||(\Sigma - \tfrac{1}{\rho}\mathbf{I})^{1/2}\Delta\boldsymbol{c}||_2\,||\widetilde{\boldsymbol{v}}||_2 \end{aligned} \tag{40}$$

where the second inequality is an application of the Cauchy-Schwartz inequality [15]. This can also be written as

$$\begin{aligned} ||\widetilde{\boldsymbol{v}}||_2^2 \;&\geq\; \tfrac{1}{4\sigma_v^2}\Delta\boldsymbol{c}^H(\Sigma - \tfrac{1}{\rho}\mathbf{I})\Delta\boldsymbol{c} \\ &=\; \tfrac{1}{4\sigma_v^2\rho}\left(\Delta\boldsymbol{c}^H\rho\Sigma\Delta\boldsymbol{c} - \Delta\boldsymbol{b}^H\Delta\boldsymbol{b}\right)\,. \end{aligned} \tag{41}$$

The instantaneous channel capacity is $C(\mathbf{H}) = \ln\det(\mathbf{I} + \rho\mathbf{H}^H\mathbf{H}) = \ln\det(\rho\Sigma)$. Σ being diagonal, Jensen's inequality leads to

$$\begin{aligned} \tfrac{1}{N_t}\Delta\boldsymbol{c}^H(\rho\Sigma)\Delta\boldsymbol{c} &\geq (\textstyle\prod_{i=1}^{N_t} \rho\,\sigma_i\,|\Delta\boldsymbol{c}_i|^2)^{\frac{1}{N_t}} \\ &= e^{\frac{C(\mathbf{H})}{N_t}}(\textstyle\prod_{i=1}^{N_t}|\Delta\boldsymbol{c}_i|^2)^{\frac{1}{N_t}}. \end{aligned} \tag{42}$$

Now consider a Tx scheme in which the transmitted rate varies with SNR. The different components of $\boldsymbol{b}_k$ come from the same QAM constellation of size $(2M)^2 = \rho^{\frac{r}{N_t}}$, $(r \geq 0)$ where $R(\rho) = r\ln\rho$ is the overall allocated rate[2] and M is a positive integer. The minimum distance of the constellation is $2d$, with $d^2 = \frac{3\sigma_b^2}{2(\rho^{\frac{r}{N_t}}-1)}$. So the components $\boldsymbol{b}_i$, $i = 1,\ldots,N_t$ of $\boldsymbol{b}$ belong to the QAM constellation $d(l + j\,p)$, $l,p \in \{-2M+1, -2M+3,\ldots,2M-1\} = \{2(l-M)+1,\, l = 0,1,\ldots,2M-1\}$. The error components $\Delta\boldsymbol{b}_i$ of $\Delta\boldsymbol{b}$ then belong to the set $2d(l' + j\,p')$, $l',p' \in \{-2M+1,-2M+2,\ldots,2M-1\} = \{-(2M-1)+l,\, l = 0,1,\ldots,4M-2\}$. This leads to the upper bound

$$\Delta\boldsymbol{b}^H\Delta\boldsymbol{b} \leq N_t 4d^2((2M-1)^2 + (2M-1)^2) \leq 8d^2 N_t \rho^{\frac{r}{N_t}}\ . \tag{43}$$

On the other hand the choice of $\mathbf{Q}$ ensures that [5]

$$(\prod_{i=1}^{N_t}|\Delta\boldsymbol{c}_i|^2)^{\frac{1}{N_t}} \geq \frac{4d^2}{N_t}\ . \tag{44}$$

Applying the bounds (42), (43), (44) to (41), leads to

$$\begin{aligned} ||\widetilde{\boldsymbol{v}}||_2^2 &\geq \tfrac{1}{4\sigma_v^2\rho}\left(N_t(e^{\frac{C(H)}{N_t}}\tfrac{4d^2}{N_t}) - 8d^2N_t\rho^{\frac{r}{N_t}}\right) \\ &= \tfrac{d^2}{\sigma_v^2\rho}\left(e^{\frac{C(H)}{N_t}} - 2N_t\rho^{\frac{r}{N_t}}\right) \\ &= \tfrac{3}{2(\rho^{\frac{r}{N_t}}-1)}\left(e^{\frac{C(H)}{N_t}} - 2N_t\rho^{\frac{r}{N_t}}\right) \\ &= \tfrac{3}{2(1-\rho^{-\frac{r}{N_t}})}\left(e^{\frac{C(H)-r\ln\rho}{N_t}} - 2N_t\right) = \gamma(\mathbf{H})\ . \end{aligned} \tag{45}$$

For a given channel realization, the error event E_1 is included in the event described by (45), hence

$$P(E_1|\mathbf{H}) \;\leq\; P\left(||\widetilde{\boldsymbol{v}}||_2^2 \geq \gamma(\mathbf{H})\,|\,\mathbf{H}\right)\ . \tag{46}$$

The normalized symbol error $\widetilde{\boldsymbol{v}}$, which is $\widetilde{\boldsymbol{v}}_k$ for $k = 1$, can be written as

$$\begin{aligned} \widetilde{\boldsymbol{v}}_k &= \mathbf{C}_{\widetilde{\boldsymbol{e}}\widetilde{\boldsymbol{e}}}^{\sharp/2}\widetilde{\boldsymbol{e}}_k \;=\; \widetilde{\boldsymbol{v}}_k^{(1)} \;+\; \widetilde{\boldsymbol{v}}_k^{(2)} \\ &= \underbrace{\mathbf{C}_{\widetilde{\boldsymbol{e}}\widetilde{\boldsymbol{e}}}^{\sharp/2}\mathbf{M}^{-1}\,\mathbf{B}^{-\dagger}(q)\mathbf{G}^{\dagger}(q)\;\boldsymbol{v}_k}_{\widetilde{\boldsymbol{v}}_k^{(1)}}\;\underbrace{-\frac{1}{\rho}\,\mathbf{C}_{\widetilde{\boldsymbol{e}}\widetilde{\boldsymbol{e}}}^{\sharp/2}\,\mathbf{M}^{-1}\,(\mathbf{B}^{-\dagger}(q)-I)\;\boldsymbol{b}_k}_{\widetilde{\boldsymbol{v}}_k^{(2)}}\ . \end{aligned} \tag{47}$$

[2]The actual rate is $R(\rho) = (1-\frac{N_t-1}{T})\,r\,\ln\rho$ as already commented on earlier.

$\widetilde{\boldsymbol{v}}_1^{(2)}$ can be written as $\widetilde{\boldsymbol{v}}_1^{(2)} = -\frac{1}{\rho}\mathbf{C}^{\sharp/2}_{\widetilde{\boldsymbol{e}}\widetilde{\boldsymbol{e}}}\mathbf{M}^{-1}\,\overline{\mathbf{B}}\,\overline{\boldsymbol{b}}_1$ where $\overline{\mathbf{B}} = [\mathbf{B}_1|\mathbf{B}_2|\ldots|\mathbf{B}_{N_t-1}]$ and $\overline{\boldsymbol{b}}_1 = [\boldsymbol{b}_2^T\,\boldsymbol{b}_3^T\ldots\boldsymbol{b}_{N_t}^T]^T$. By construction of vector norm induced matrix norm [15], $||\widetilde{\boldsymbol{v}}_1^{(2)}||_2 \le ||\frac{\sigma_b}{\rho}\,\mathbf{C}^{\sharp/2}_{\widetilde{\boldsymbol{e}}\widetilde{\boldsymbol{e}}}\mathbf{M}^{-1}\,\overline{\mathbf{B}}||_2\;||\frac{1}{\sigma_b}\overline{\boldsymbol{b}}_1||_2$. Now, on the one hand,

$$\begin{aligned}(\tfrac{\sigma_b}{\rho}\mathbf{C}^{\sharp/2}_{\widetilde{\boldsymbol{e}}\widetilde{\boldsymbol{e}}}\mathbf{M}^{-1}\,\overline{\mathbf{B}})(\tfrac{\sigma_b}{\rho}\mathbf{C}^{\sharp/2}_{\widetilde{\boldsymbol{e}}\widetilde{\boldsymbol{e}}}\mathbf{M}^{-1}\,\overline{\mathbf{B}})^H &= \mathrm{E}\widetilde{\boldsymbol{v}}_1^{(2)}\widetilde{\boldsymbol{v}}_1^{(2)H}\\ &\le \mathrm{E}\widetilde{\boldsymbol{v}}_1^{(1)}\widetilde{\boldsymbol{v}}_1^{(1)H} + \mathrm{E}\widetilde{\boldsymbol{v}}_1^{(2)}\widetilde{\boldsymbol{v}}_1^{(2)H} = \mathrm{E}\widetilde{\boldsymbol{v}}_1\widetilde{\boldsymbol{v}}_1^H \le I\,.\end{aligned} \tag{48}$$

Consequently $||\frac{\sigma_b}{\rho}\,\mathbf{C}^{\sharp/2}_{\widetilde{\boldsymbol{e}}\widetilde{\boldsymbol{e}}}\mathbf{M}^{-1}\,\overline{\mathbf{B}}||_2 \le 1$. On the other hand, all the components of $\overline{\boldsymbol{b}}_1$ belong to the same QAM constellation, hence

$$\begin{aligned}||\tfrac{1}{\sigma_b}\overline{\boldsymbol{b}}_1||_2^2 &\le \tfrac{1}{\sigma_b^2}N_t(N_t-1)2d^2(2M-1)^2\\ &= 3N_t(N_t-1)\tfrac{(2M-1)^2}{(2M)^2-1} \le 3N_t(N_t-1) = \gamma_1^2\,.\end{aligned} \tag{49}$$

We conclude that $||\widetilde{\boldsymbol{v}}_1^{(2)}||_2 \le \gamma_1$. Now, by the triangle inequality [15], we get $||\widetilde{\boldsymbol{v}}_1||_2 \le ||\widetilde{\boldsymbol{v}}_1^{(1)}||_2 + ||\widetilde{\boldsymbol{v}}_1^{(2)}||_2 \le ||\widetilde{\boldsymbol{v}}_1^{(1)}||_2 + \gamma_1$. Upper bound (46) now leads to

$$P(E_1|\mathbf{H}) \le P\left(||\widetilde{\boldsymbol{v}}_1^{(1)}||_2^2 \ge \gamma_2(\mathbf{H})\,|\,\mathbf{H}\right) \tag{50}$$

where $\gamma_2(\mathbf{H}) = (\sqrt{\gamma(\mathbf{H})} - \gamma_1)^2$. $\widetilde{\boldsymbol{v}}_1^{(1)}$ has a zero mean Gaussian distribution, with a bounded covariance matrix $\mathbf{C}_{\widetilde{\boldsymbol{v}}^{(1)}\widetilde{\boldsymbol{v}}^{(1)}} \le I_{N_t}$, by a reasoning similar to the one in (48), and with rank equal to p. Let $\mathbf{W}$ be a $N_t \times p$ matrix of rank p such that $\mathbf{C}_{\widetilde{\boldsymbol{v}}^{(1)}\widetilde{\boldsymbol{v}}^{(1)}} = \mathbf{W}\,\mathbf{W}^H \le I_{N_t}$. Denote $\boldsymbol{n} = \mathbf{W}^\sharp\widetilde{\boldsymbol{v}}_1^{(1)}$ where $\mathbf{W}^\sharp = (\mathbf{W}^H\mathbf{W})^{-1}\mathbf{W}^H$. Then $\boldsymbol{n}$ is Gaussian with zero mean and covariance matrix $\mathbf{C}_{\boldsymbol{n}\boldsymbol{n}} = I_p$. Also $\mathbf{W}\,\mathbf{W}^H \le I_{N_t}$ implies $\mathbf{W}^H\mathbf{W} \le I_p$, and since $\widetilde{\boldsymbol{v}}_1^{(1)} = \mathbf{W}\,\boldsymbol{n}$, we get

$$||\widetilde{\boldsymbol{v}}_1^{(1)}||_2^2 = \boldsymbol{n}^H\,\mathbf{W}^H\mathbf{W}\,\boldsymbol{n} \le ||\boldsymbol{n}||_2^2\,. \tag{51}$$

From (50), the error probability is then majorized by

$$P(E_1|\mathbf{H}) \;\le\; P(||\boldsymbol{n}||_2^2 \ge \gamma_2(\mathbf{H})\,|\,\mathbf{H})\,. \tag{52}$$

So the main idea in the probablity of error analysis without Gaussian assumption is that in the normalized error, the contribution of the residual ISI is finite, whereas for any rate below capacity, an error events gets situated in an exponentially receding tail of the Gaussian noise part.

For the last $N_t{-}1$ symbol periods of the frame, less symbols appear in the residual ISI and as a result γ_1 gets reduced to $\gamma_1^{'}$ and γ_2 gets increased to $\gamma_2^{'}$, hence

$$P(E_1|\mathbf{H}) \;\le\; P(||\boldsymbol{n}||_2^2 \ge \gamma_2^{'}(\mathbf{H})\,|\,\mathbf{H}) \;\le\; P(||\boldsymbol{n}||_2^2 \ge \gamma_2(\mathbf{H})\,|\,\mathbf{H}) \tag{53}$$

which leads to the second part of (29), at least for the asymptotic analysis considered here.

Step 3:

In step 3 we seek to study the behavior of the error probability for large SNR, in order to derive the diversity-vs-multiplexing tradeoff achieved by the proposed scheme. Let λ_i, $i = 1, \ldots, p$, be the nonzero eigenvalues of $\mathbf{H}^H\mathbf{H}$ sorted in a nondecreasing order. We continue in the footsteps of [1] and introduce the variables α_i via $\lambda_i = \rho^{-\alpha_i}$. At high SNR we have $(1+\rho\lambda_i) \doteq \rho^{(1-\alpha_i)^+}$, where $(x)^+$ denotes $\max\{0, x\}$. On the other hand the capacity satisfies $C(\mathbf{H}) = \sum_{i=1}^{p} \ln(1+\rho\lambda_i)$, hence $e^{C(\mathbf{H})} \doteq \rho^{\sum_{i=1}^{p}(1-\alpha_i)^+}$. In [1], it was shown that for an allocated rate $r \ln \rho$, the outage probability is

$$P(outage) \doteq P(\sum_{i=1}^{p}(1-\alpha_i)^+ \leq r) \doteq \rho^{-d_{out}(r)}, \tag{54}$$

where $d_{out}(r)$ is given by the piecewise-linear function connecting the points $(k, d_{out}(k))$, $k = 0, 1, \ldots, p$, where

$$d_{out}(k) = (p-k)(q-k)\ . \tag{55}$$

It was also shown in the same reference that any scheme with rate $R(\rho) = r \ln \rho$ has an error probability that satisfies

$$P_e \dot{\geq} \rho^{-d_{out}(r)}, \tag{56}$$

hence $d_{out}(r) = d^*(r)$ is also called the optimal diversity-rate tradeoff curve. Let $\epsilon \in (0, p)$. We define the $outage_\epsilon$ event as $\sum_{i=1}^{p}(1-\alpha_i)^+ \leq r+\epsilon$. The complementary event of $outage_\epsilon$ is denoted as $no\, outage_\epsilon$. An upper bound on $P(E_1)$ can now be derived as

$$\begin{aligned} P(E_1) &\leq P(\{outage_\epsilon\} \cup E_1) \\ &= P(outage_\epsilon) + P(E_1, no\, outage_\epsilon). \end{aligned} \tag{57}$$

since

$$\{outage_\epsilon\} \cup E_1 = \{outage_\epsilon\} \cup (\{no\, outage_\epsilon\} \cap E_1)\ . \tag{58}$$

From (54) we conclude that

$$P(outage_\epsilon) \doteq P\left(\sum_{i=1}^{p}(1-\alpha_i)^+ \leq r+\epsilon\right) \doteq \rho^{-d_{out}(r+\epsilon)}\ . \tag{59}$$

Let's characterize $P(E_1, no\, outage_\epsilon)$. By applying the Chernoff bound to (52), we get for any $\lambda \in (0,1)$

$$\begin{aligned} P(E_1,\, no\, outage_\epsilon) &= \int_{no\, outage_\epsilon} P(E_1|\mathbf{H})\, f(\mathbf{H})\, d\mathbf{H} \\ &\leq \int_{no\, outage_\epsilon} P(||\boldsymbol{n}||_2^2 \geq \gamma_2(\mathbf{H})|\mathbf{H})\, f(\mathbf{H})\, d\mathbf{H} \\ &\leq \int_{no\, outage_\epsilon} (1-\lambda)^{-N_t} e^{-\lambda\gamma_2(\mathbf{H})}\, f(\mathbf{H})\, d\mathbf{H}\, . \end{aligned} \tag{60}$$

In particular for $\lambda = \frac{1}{2}$

$$P(E_1,\, no\, outage_\epsilon) \leq \int_{no\, outage_\epsilon} 2^{N_t} e^{-\frac{\gamma_2(\mathbf{H})}{2}}\, f(\mathbf{H})\, d\mathbf{H}\, . \tag{61}$$

For any channel realization, the event $no\, outage_\epsilon$ means $\sum_{i=1}^p (1-\alpha_i)^+ > r+\epsilon$, or hence $e^{\frac{C-r\,\ln\rho}{N_t}} \doteq \rho^{\frac{1}{N_t}(\sum_{i=1}^p(1-\alpha_i)^+ - r)} \dot{>} \rho^{\frac{\epsilon}{N_t}}$. Introducing the definition of γ_2 then into (61) leads to

$$\begin{aligned} P(E_1,\, no\, outage_\epsilon) &\dot{\leq} 2^{N_t}\, e^{-\frac{1}{2}\left(\left(\frac{3}{2(1-\rho^{-\frac{r}{N_t}})}(\rho^{\frac{\epsilon}{N_t}} - 2N_t)\right)^{\frac{1}{2}} - \gamma_1\right)^2} \int_{no\, outage_\epsilon} f(\mathbf{H})\, d\mathbf{H} \\ &\dot{\leq} 2^{N_t}\, e^{-\frac{1}{2}\left(\left(\frac{3}{2(1-\rho^{-\frac{r}{N_t}})}(\rho^{\frac{\epsilon}{N_t}} - 2N_t)\right)^{\frac{1}{2}} - \gamma_1\right)^2} = \gamma_\epsilon(\rho)\, . \end{aligned} \tag{62}$$

Now $\lim_{\rho\to\infty} \frac{\ln \gamma_\epsilon(\rho)}{\ln \rho} = -\infty$ for any $\epsilon > 0$. Hence for any finite y we have $P(E_1,\, no\, outage_\epsilon) \dot{\leq} \rho^{-y}$, and by consequence

$$P(E_1,\, no\, outage_\epsilon) \dot{\leq} \rho^{-d_{out}(r+\epsilon)}\, . \tag{63}$$

Combining this result with (57) and (59) leads to

$$P(E_1) \dot{\leq} \rho^{-d_{out}(r+\epsilon)}\, . \tag{64}$$

This is valid for any $\epsilon > 0$, hence

$$P(E_1) \dot{\leq} \rho^{-d_{out}(r)} = \rho^{-d^*(r)}\, . \tag{65}$$

Using (35), we arrive at an upper bound for the frame error probability

$$P_e \dot{\leq} \rho^{-d^*(r)}\, . \tag{66}$$

Combined with the lower bound of (56), this allows us to conclude that the proposed scheme attains the optimal diversity-vs-multiplexing tradeoff, i.e.

$$P_e \doteq \rho^{-d^*(r)}\, . \tag{67}$$

□

It is actually possible to extend this result to any number of transmit antennas.

Theorem 3: *The use of a weighted minimum distance detector and QAM constellations allows the Conventional MIMO DFE Rx, with* **UMMSE design**, *to achieve the optimal diversity-vs-multiplexing tradeoff for any number of transmit antennas N_t.*

Proof : Theorem 2 showed that the UMMSE Conventional MIMO DFE achieves the optimal tradeoff for $N_t = 2^n$ with n integer. The proof of Theorem 2 can be extended to the case of $N_t \neq 2^n$ by using a number of data streams $N_s = 2^{\lceil \log_2 N_t \rceil}$ and a precoding matrix $\mathbf{Q}$ that contains only the first N_t rows of $\mathbf{Q}_{N_s}$

$$\mathbf{Q}_{N_s} = \frac{1}{\sqrt{N_s}} \begin{bmatrix} 1 & \theta_1 & \dots & {\theta_1}^{N_s-1} \\ 1 & \theta_2 & \dots & {\theta_2}^{N_s-1} \\ \vdots & \vdots & & \vdots \\ 1 & \theta_{N_s} & \dots & {\theta_{N_s}}^{N_s-1} \end{bmatrix}, \tag{68}$$

where now the θ_i are the roots of $\theta^{N_s} - j = 0\,,\; j = \sqrt{-1}$. The overall channel is $\mathbf{G}(z) = \mathbf{H}\,\mathbf{D}(z)\,\mathbf{Q}$. One can now introduce a virtual channel $\mathbf{H}_s$ of size $N_r \times N_s$, that contains $\mathbf{H}$ in the first N_t columns and zeros in the remaining columns: $\mathbf{H}_s = [\mathbf{H} \mid 0_{N_r \times (N_s - N_t)}]$. This leads to $\mathbf{G}(z) = \mathbf{H}_s\,\mathbf{D}_{N_s}(z)\,\mathbf{Q}_{N_s}$ where $\mathbf{D}_{N_s}(z)$ is the delay diversity matrix of size $N_s \times N_s$. Using this embedding, steps 1 and 3 of the proof of Theorem 2 remain unchanged, whereas for step 2 N_t should be replaced by $N_s = 2^{\lceil \log_2 N_t \rceil}$. □

B. Case of MMSE ZF DFE Design

Theorem 4: *In the case of a frequency-flat channel and $N_r \geq N_t$, $N_t = 2^n$ (n integer), the use of a weighted minimum distance detector and QAM constellations (for the streams $b_{m,k}$) allows the Conventional MIMO DFE Rx, with* **MMSE ZF design**, *to achieve the diversity-vs-multiplexing tradeoff given by $d^{ZF}(r)$. The tradeoff $d^{ZF}(r)$ is the piecewise-linear function connecting the points $(k, d^{ZF}(k))$, $k = 0, \dots, N_t$, with*

$$d^{ZF}(k) = \frac{N_t - k}{2}(2N_r - N_t - k + 1)\,. \tag{69}$$

The tradeoff of the MMSE-ZF DFE gets compared to that of the MMSE DFE in Fig. 3.

Proof : The proof of Theorem 4 follows the same lines as the proof of Theorem 2. We point out below the minor differences.

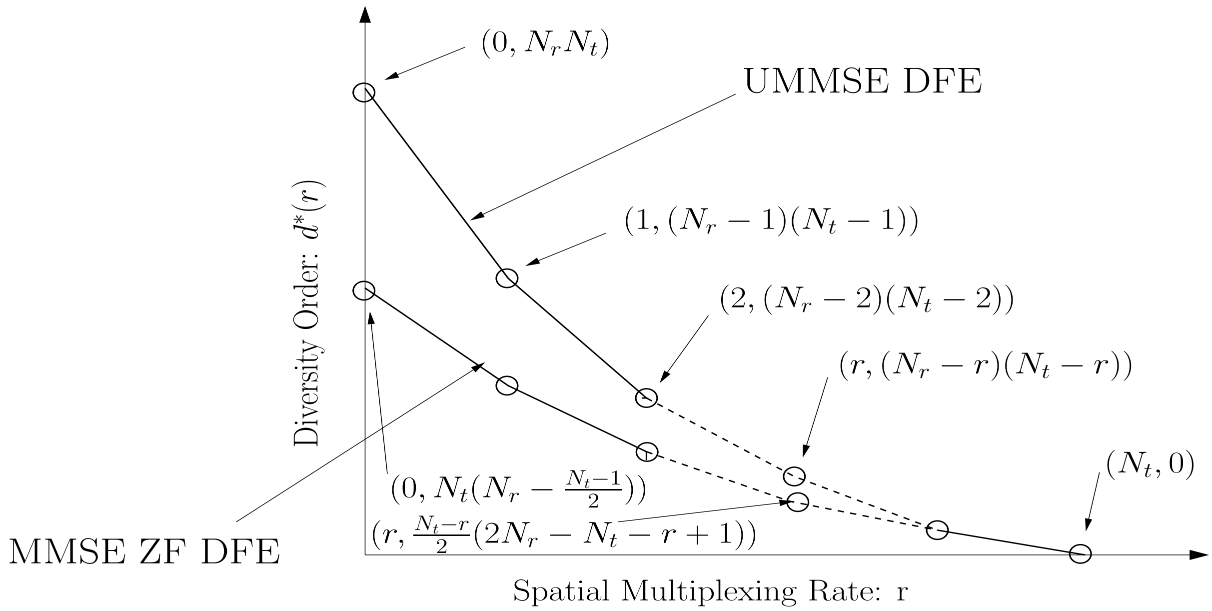

Fig. 3. Diversity-vs-Multiplexing tradeoff comparison between MMSE and MMSE-ZF DFE designs (assuming $N_r \geq N_t$).

Step 1:

This step is the same as step 1 of Theorem 2, its main result is

$$P_e \doteq P(E_1) \,. \tag{70}$$

Step 2:

As we have established in step 2 for Theorem 2, an error occurs when detecting the first symbol if $\Delta\boldsymbol{b}^H\mathbf{M}\,\Delta\boldsymbol{b} \leq 2\,\Re\{\Delta\boldsymbol{b}^H\mathbf{M}\,\boldsymbol{e}_1\}$ where $\mathbf{M} = \mathbf{Q}^H\mathbf{D}\mathbf{Q}$, $\Delta\boldsymbol{b} = \boldsymbol{b}_1 - \boldsymbol{b}_1'$, $\Delta\boldsymbol{c} = \mathbf{Q}\,\Delta\boldsymbol{b}$ and $\widetilde{\boldsymbol{v}}_1 = \sigma_v^{-1}\mathbf{D}^{1/2}\mathbf{Q}\,\boldsymbol{e}_1$ (see section II-B). Unlike in the MMSE design, the MMSE ZF Conventional MIMO DFE makes no compromise between interference cancellation and noise enhancement, and cancels the interference entirely. Hence $\widetilde{\boldsymbol{v}}_1$ has a Gaussian distribution $\widetilde{\boldsymbol{v}}_1 \sim \mathcal{CN}(\prime, \mathbf{I}_{\mathcal{N}_\sqcup})$. Again using the Cauchy-Swartz inequality we get

$$\Delta\boldsymbol{c}^H\mathbf{D}\,\Delta\boldsymbol{c} \leq 2\,\sigma_v||\mathbf{D}^{1/2}\Delta\boldsymbol{c}||_2\,||\widetilde{\boldsymbol{v}}_1||_2\,, \tag{71}$$

which can also be written as

$$\begin{aligned} ||\widetilde{\boldsymbol{v}}_1||_2^2 &\geq \frac{1}{4\sigma_v^2}\,\Delta\boldsymbol{c}^H\mathbf{D}\,\Delta\boldsymbol{c} \\ &= \frac{1}{4\sigma_v^2\rho}\left(\Delta\boldsymbol{c}^H(\mathbf{I}+\rho\mathbf{D})\,\Delta\boldsymbol{c} - \Delta\boldsymbol{b}^H\Delta\boldsymbol{b}\right)\,. \end{aligned} \tag{72}$$

Let $e^{\beta(H)} = \prod_{i=1}^{N_t}(1+\rho\mathbf{D}_{ii}) = \det(\mathbf{I}+\rho\mathbf{D})$. Using Jensen's inequality we get

$$\frac{1}{N_t}\Delta\boldsymbol{c}^H(\mathbf{I}+\rho\mathbf{D})\Delta\boldsymbol{c} \,\geq\, e^{\frac{\beta(H)}{N_t}}\left(\prod_{i=1}^{N_t}|\Delta\boldsymbol{c}_i|^2\right)^{\frac{1}{N_t}}\,. \tag{73}$$

As in the proof of Theorem 2, the error event can be shown to be included in the following event

$$||\widetilde{\boldsymbol{v}}_1||_2^2 \geq \frac{3}{2(1-\rho^{-\frac{r}{N_t}})}\left(e^{\frac{\beta(H)-r\ln\rho}{N_t}} - 2N_t\right) = \gamma(H) \ . \tag{74}$$

Step 3:

$N_r \geq N_t$ is required for the MMSE ZF design to hold. $\mathbf{D}$ is identifiable from the QR factorization of $\mathbf{H} = \mathbf{UR}$. In fact, $\mathbf{U}$ is a $N_r \times N_t$ unitary matrix and $\mathbf{R}$ is a $N_t \times N_t$ upper triangular matrix, and also $\mathbf{LDL}^H = \mathbf{R}^H\mathbf{R}$ with $\mathbf{D}_{ii} = |\mathbf{R}_{ii}|^2$. Denote $\mathbf{h}_{1:i} = [\mathbf{h}_1 \ldots, \mathbf{h}_i]$ where $\mathbf{h}_i$ is column i of $\mathbf{H}$, and $\overline{\mathbf{h}}_i = P^{\perp}_{\mathbf{h}_{1:i-1}}\mathbf{h}_i$ the projection of $\mathbf{h}_i$ onto the orthogonal complement of $\mathbf{h}_{1:i-1}$. Then $|\mathbf{R}_{ii}| = ||\overline{\mathbf{h}}_i||_2$ and $\mathbf{D}_{ii} = ||\overline{\mathbf{h}}_i||_2^2 = \overline{\mathbf{h}}_i^H\overline{\mathbf{h}}_i$.

$\beta(H)$ has been reported in [1] to be the instantaneous capacity of the BLAST technique. The α_i get introduced via $\mathbf{D}_{ii} = \rho^{-\alpha_i}$, $i = 1, \ldots, N_t$. Paralleling the steps in [1], an outage event occurs for $\sum_{i=1}^{N_t}(1-\alpha_i)^+ \leq r$. In [1], it has been shown that $P(outage) \doteq \rho^{-d_{out}^{ZF}(r)}$, where $\doteq$ denotes the exponential equality. $d_{out}^{ZF}(r)$ is the piecewise-linear function connecting the points $(k, d_{out}^{ZF}(k))$, $k = 0, \ldots, N_t$, with

$$d_{out}^{ZF}(k) = \frac{N_t - k}{2}(2N_r - N_t - k + 1) \ . \tag{75}$$

It was also shown in the same reference that any scheme with rate $R(\rho) = r\ln\rho$, and a ZF constrained structure, has an error probability that satisfies

$$P_e \dot{\geq} \rho^{-d_{out}^{ZF}(r)} \ . \tag{76}$$

The rest of the proof is the same as for Theorem 2, apart that $P(E_1|\mathbf{H})$ is upper bounded by

$$\begin{aligned} P(E_1|\mathbf{H}) &\leq P(||\widetilde{\boldsymbol{v}}_1||_2^2 \geq \gamma(\mathbf{H})|\mathbf{H}) \\ &\leq 2^{N_t}\, e^{-\frac{\gamma(H)}{2}} \ . \end{aligned} \tag{77}$$

In the end we conclude that $P_e \doteq \rho^{-d_{out}^{ZF}(r)}$ and

$$d^{ZF}(r) = d_{out}^{ZF}(r) \ . \tag{78}$$

□

IV. Concluding Remarks

In this paper we showed again, be it for the specific transmission problem and equalizer considered here, that even though a MMSE design tends to the corresponding MMSE ZF design at high SNR, those two designs have a substantially different behavior from a diversity point of view, even though diversity is characterized at high SNR. Furthermore, MMSE designs also apply to scenarios in which zero forcing is not possible. For finite SNR, it may be desirable to robustify the transmission scheme against error propagation by combining it with error correcting codes [11], [12], [16].

The introduction of a DFE reduces the cascade of prefilter, frequency-flat channel and DFE to a frequency-flat MIMO system again, leading to the joint detection of a vector of symbols of size N_t (when it is a power of two). We conjecture that the complexity of this detection problem constitutes a lower bound for the complexity of MIMO transceiver schemes attaining the optimal diversity-vs-multiplexing tradeoff.

We may also remark that even though the space-time spreading transmission scheme considered here is easily extended to the frequency fading channel case [14], the use of a DFE to attain the optimal tradeoff is not so clear. What happens in the frequency-flat case is that the feedforward and feedback filters of the DFE are simple functions of the prefilter $\mathbf{T}(z)$ and the channel $\mathbf{H}$ separately and do not require to consider the cascade $\boldsymbol{G}(z)$. This separation property disappears in the frequency fading case.

References

[1] L. Zheng and D. Tse, "Diversity and Multiplexing: a Fundamental Tradeoff in Multiple-Antenna Channels," *IEEE Trans. Info. Theory*, vol. 49, no. 5, pp. 1073–1096, May 2003.

[2] H. Yao and G.W. Wornell, "Achieving the Full MIMO Diversity-Multiplexing Frontier with Rotation-Based Space-Time Codes," in *Proc. 41th Annual Allerton Conference on Communication, Control, and Computing*, Monticello, Illinois, Oct. 2003.

[3] S. Tavildar and P. Viswanath, "Permuation Codes: Achieving the Diversity-Multiplexing Tradeoff," in *IEEE ISIT 2004*, Chicago, Illinois, Jun-Jul 2004.

[4] H. El Gamal, G. Caire, and M.O. Damen, "Lattice Coding and Decoding Achieve the Optimal Diversity-vs-Multiplexing Tradeoff of MIMO Channels," *IEEE Trans. Information Theory*, June 2004.

[5] A. Medles and D.T.M. Slock, "Linear Convolutive Space-Time Precoding for Spatial Multiplexing MIMO Systems," in *Proc. 39th Annual Allerton Conference on Communication, Control, and Computing*, Monticello, Illinois, Oct. 2001.

[6] A. Medles and D.T.M. Slock, "Multistream Space-Time Coding by Spatial Spreading, Scrambling and Delay Diversity," in *Proc. ICASSP Conf.*, Orlando, FL, May 2002.

[7] H. EL Gamal and R. Hammons, "A new approach to layered space-time coding and signal processing," *IEEE Trans. Info. Theory*, vol. 47, no. 6, pp. 2321–2334, Sept. 2001.

[8] E. Boutillon X. Giraud and J.C. Belfiore, "Algebraic Tools to Build Modulation Schemes for Fading Channels," *IEEE Trans. Info. Theory*, vol. 43, no. 3, pp. 938–952, May 1997.

[9] B. Hassibi and B. M. Hochwald, "High-Rate Codes that are Linear in Space and Time," *IEEE Trans. Info. Theory*, vol. 48, no. 7, pp. 1804 –1824, August 2000.

[10] S. Galliou and J.C. Belfiore, "A New Familly of Linear Full-Rate Space-Time Codes Based on Galois Theory," in *Proc. IEEE ISIT 2002*, Lausane, Switzerland, Jun-Jul 2002.

[11] T. Guess and M. Varanasi, "A New Successively Decodable Coding Technique for Intersymbol-Interference Channels," in *Proc. IEEE ISIT*, Sorrento, Italy, June 2000.

[12] M. Kobayashi and G. Caire, "A Low Complexity Approach to Space-Time Coding for Multipath Channels," in *Proc. 6th Int'l Symp. on Wireless Personal Multimedia Communications*, Yokosuka, Japan, Oct 2003.

[13] A. Duel-Hallen, "Equalizers for Multiple Input/Multiple Output Channels and PAM Systems with Cyclostationary Input Sequences," *IEEE J. Select. Areas Comm.*, vol. 10, pp. 630–639, Apr. 1992.

[14] A. Medles and D.T.M. Slock, "Spatial Multiplexing by Spatiotemporal Spreading of Multiple Symbol Streams," in *Proc. The 5th IEEE Int'l Symp. Wireless Personal Multimedia Comm's (WPMC)*, Honolulu, Hawaii, Oct. 2002.

[15] G.H. Golub and C.F. Van Loan, *Matrix Computations*, The Johns Hopkins University Press, 3rd edition, 1996.

[16] A. Medles and D.T.M. Slock, "Linear versus Channel Coding Trade-Offs in Full Diversity Full Rate MIMO Systems," in *Proc. ICASSP Conf.*, Montreal, CAN, May 2004.